Supplementary Materials

First-Principles Study of Band alignment in Passivated and Doped GaN/WSe_2 van der Waals Heterojunctions

Xiurui Lv[1], Guijuan Zhao[1], Yinghui Xie[1], Haiyan Wu[1], Jianhong Yang[1], Desheng Xue[1] and Guipeng Liu [1, a)]

[1]School of Physical Science and Technology, Lanzhou University, Lanzhou 730000, China.

[a)]Author to whom correspondence should be addressed: liugp@lzu.edu.cn (Guipeng Liu)

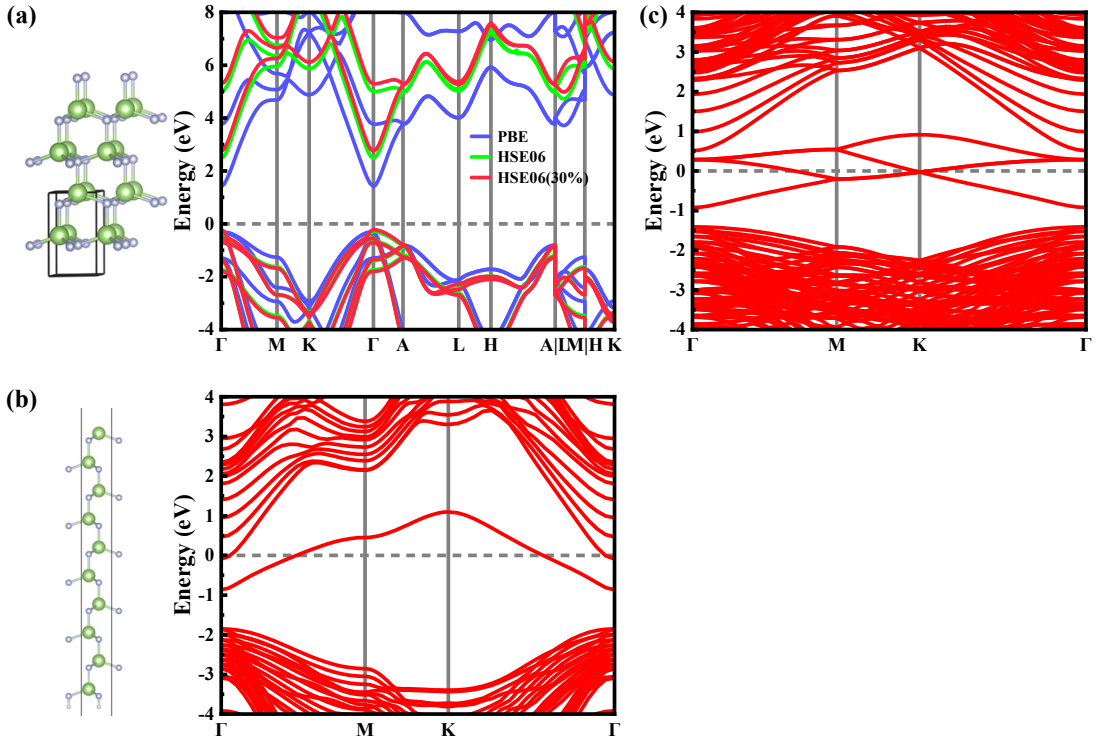

FIG. S1. (a) The crystal structure and band structure of hexagonal GaN. (b) Atomic structure and band structure of the 1 × 1 GaN (0001) surface. (c) Band structure of the 2 × 2 GaN (0001) surface. (d) Projected density of states (PDOS) for different layers of GaN on the 2 × 2 GaN surface.

Fig. S1(a) illustrates the atomic structure and band structure of GaN crystals. After structural optimisation, the obtained lattice constants are a = b = 3.218 Å and c = 5.243 Å. The bandgap values calculated using the PBE method and the HSE06 method are 1.72 eV and 2.76 eV respectively, both indicating a direct bandgap. Although the HSE06 functional improves the bandgap estimation, it still underestimates the experimental value of 3.40 eV for GaN. Increasing the hybridisation parameter further raises the bandgap value, employing a 30% hybridisation parameter yields a bandgap of 2.96 eV. The atomic and electronic structures of the GaN (1 × 1) surface are presented in Fig. S1(b), and the corresponding band structure of the (2 × 2) surface is shown in Fig. S1(c).

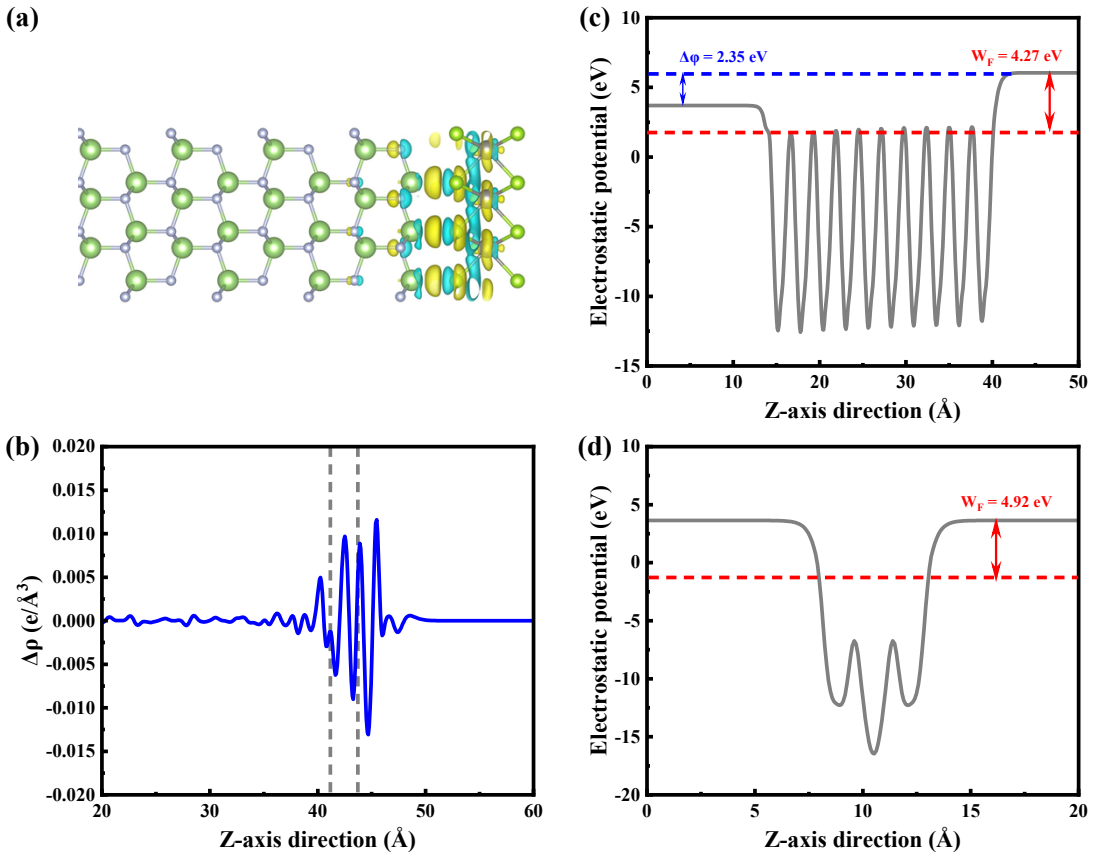

FIG. S2. (a) The charge density difference and (b) $\Delta\rho$ of GaN/WSe_2 heterojunction. Electrostatic potential energy distribution on (c) GaN surfaces and (d) strained WSe_2.

The charge density difference and $\Delta\rho$ ($\Delta\rho = \rho_{hetero} - \rho_{GaN\_surface} - \rho_{WSe_2}$) for GaN/$WSe_2$ heterojunction are presented in Fig. S2(a) and (b). Interfacial interactions induce notable charge redistribution, with a clear accumulation of electrons observable within the interlayer region. Because evaluating interlayer charge transfer solely from charge density differences is non-trivial, we further performed Bader charge analysis. The results indicate a transfer of 0.82 electrons from GaN to WSe_2, consistent with the conclusions drawn from the band structure analysis. The electrostatic potential energy distribution of the GaN surface and WSe_2 are depicted in Figs. S2(c) and (d). Within the 2×2 supercell structure, all exposed Ga atoms within the surface structure are uniformly distributed, meaning each exposed G atom contributes 0.21 electrons to the transfer. The charge differential map reveals that charge transfer predominantly occurs at exposed Ga atoms. Furthermore, analysis of the Bader charge reveals that surface-exposed Ga atoms lose approximately 0.22 electrons upon heterojunction formation, indicating that electron transfer primarily occurs at surface-state positions.

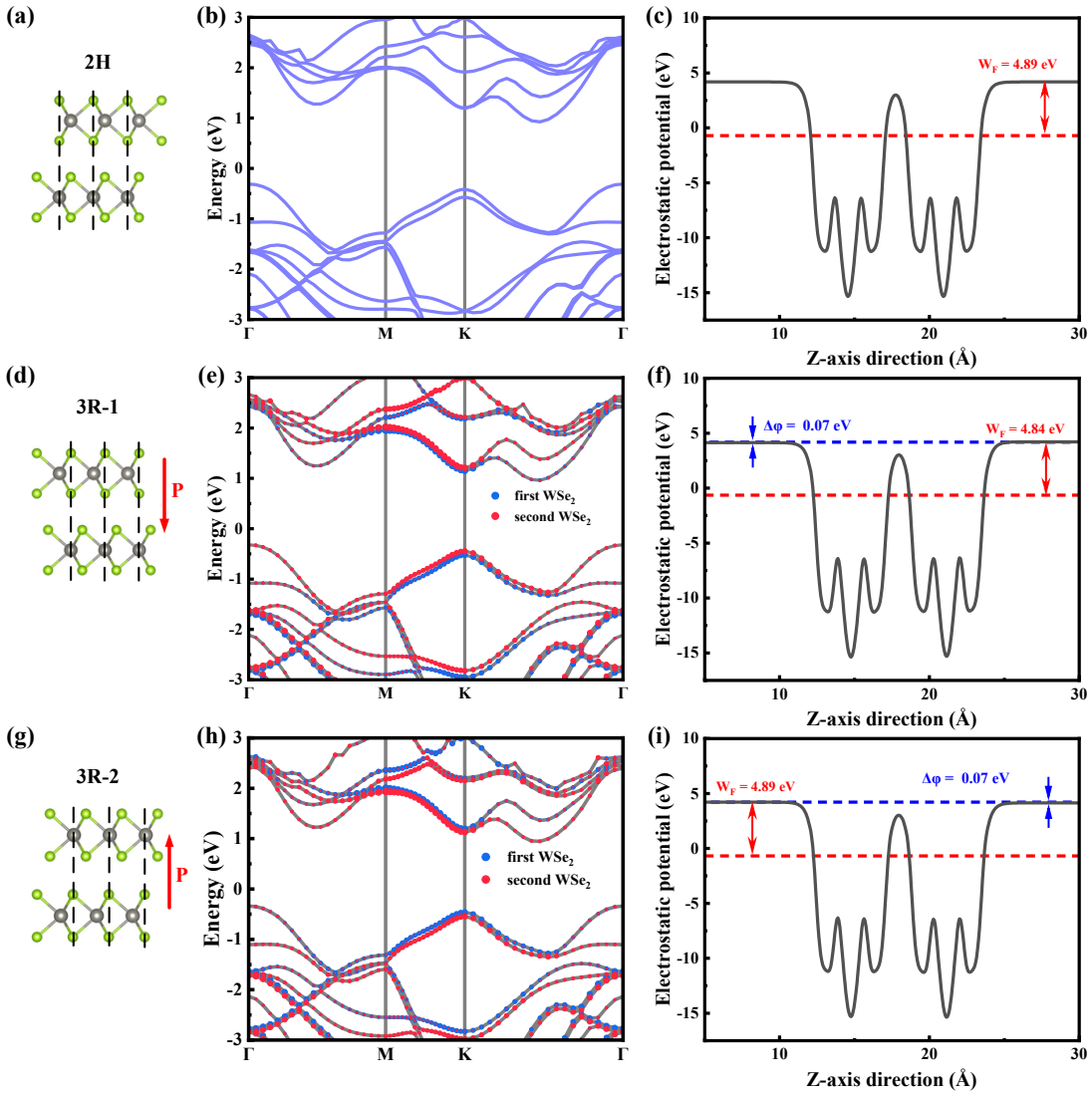

FIG. S3. Atomic structures, band structures, and electrostatic potential energy distributions of three types of bilayer WSe_2:(a)-(c) 2H-WSe_2; (d)-(f) 3R-1-WSe_2; (g)-(i) 3R-2-WSe_2.

The atomic structures, band structures, and electrostatic potential distributions of the three bilayer WSe_2 configurations are shown in Fig. S3. In the 3R stacking arrangement, a relative in-plane slip between layers breaks inversion symmetry, giving rise to slip ferroelectricity. Owing to the two possible slip directions, the 3R stack exhibits two distinct spontaneous polarization orientations; therefore, two variants, denoted 3R-1 and 3R-2, were constructed. The three stacking configurations show no significant differences in their overall band structures. However, the opposite polarization directions in 3R-1 and 3R-2 lead to different layer-resolved band contributions. In 3R-1, the energy levels associated with the first WSe_2 layer lie lower than those of the second layer, whereas in 3R-2 the order is reversed. The electrostatic potential profiles further confirm the opposite spontaneous polarization orientations in the two 3R stacking variants.

FIG. S4. EBS of the (a) $Mg_{Ga}GaN$ surface and (b) V_NGaN surface. The electrostatic potential energy distributions for the (c) $Mg_{Ga}GaN$ surface and (d) V_NGaN surface. (e) Schematic diagram of band bending in $Mg_{Ga}GaN/WSe_2$ and V_NGaN/WSe_2 heterojunctions.

The EBS of $Mg_{Ga}GaN$ and V_NGaN surfaces are shown in Figs. s4(a) and (b). The electrostatic potential energy distributions for the two heterojunctions are shown in Figs S4(c) and (d), and the corresponding band-bending diagrams are given in Fig. S4(e). The work functions of the $Mg_{Ga}GaN/WSe_2$ and V_NGaN/WSe_2 heterojunctions are 4.02 eV and 4.13 eV, respectively—values comparable to the 4.08 eV obtained for the undoped heterojunction.

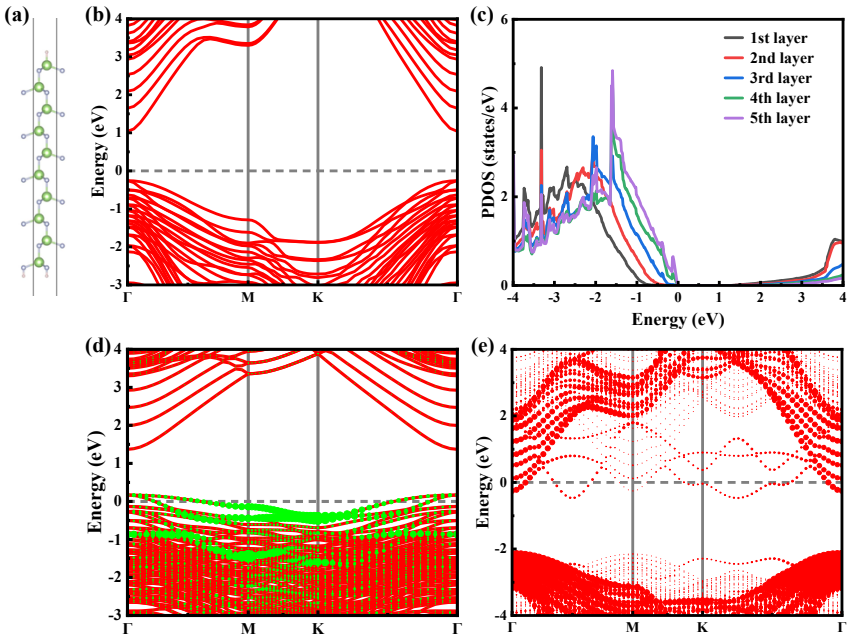

FIG. S5. (a) Atomic structure and (b) band structure of the H-GaN surface. (c) Projected density of states for GaN atoms in different layers. The band structure of (d) the H-Mg_{Ga}GaN surface and (e) H-V_NGaN surface.

Fig S5 (a)-(c) presents the atomic structure, band structure, and PDOS for layer-resolved PDOS of the H-GaN (0001) surface. The band structures of the H-Mg_{Ga}GaN and H-V_NGaN surface structures are shown in Figs S5(d) and (e). That confirm that once surface states are removed, the Fermi level shifts into the valence band for Mg-doped GaN and into the conduction band for N-vacancy GaN.

FIG. S6.The electrostatic potential energy distributions for the (a) H-GaN/WSe_2, (b) H-Mg_{Ga}GaN/WSe_2 and (c) H-V_NGaN/WSe_2. Schematic diagram of band bending in (d) H-GaN/WSe_2,

(e) H-Mg_{Ga}GaN/WSe_2 and (f) H-V_NGaN/WSe_2.

The electrostatic potential energy distribution and corresponding band-bending diagrams for the three heterojunctions are shown in Fig S6. For H-GaN/WSe_2 heterojunction, the work function is 4.95 eV, lying between that of monolayer WSe_2 (4.92 eV) and the H-GaN surface (6.51 eV). In this case, the GaN bands bend downward on both sides of the interface, whereas the WSe_2 bands bend upward. Owing to the presence of an interfacial van der Waals gap, interlayer charge transfer is strongly suppressed, resulting in relatively weak band bending. For the H-Mg_{Ga}GaN/WSe_2 heterojunction, Mg doping increases the work function of the GaN surface to 6.92 eV, which rises to 5.16 eV after forming the heterojunction. The direction of band bending remains the same as in H-GaN/WSe_2, but its magnitude increases due to the enhanced work-function contrast. For H-V_NGaN/WSe_2, N vacancies decrease the GaN surface work function to 3.42 eV, which is lower than that of WSe_2. This reverses the band-bending polarity: the GaN bands bend upward at the interface, while the WSe_2 bands bend downward.